Honda Research Institute EU
Honda Research Institute Europe GmbH
https://www.honda-ri.de/

Evolvability as Concept for the Optimal Design of Free-Form Deformation Control Volumes

Henry Lehmann, Stefan Menzel

2012

Preprint:

This is an accepted article published in Proceedings of the 2012 IEEE Congress on Evolutionary Computation. The final authenticated version is available online at: https://doi.org/10.1109/CEC.2012.6256510

Evolvability as Concept for the Optimal Design of Free-Form Deformation Control Volumes

Henry Lehmann
Institute for Informatics, TU Bergakademie Freiberg
Bernhard-von-Cotta-Straße 2
09596 Freiberg, Germany
Email: henry.lehmann@informatik.tu-freiberg.de

Stefan Menzel
Honda Research Institute Europe GmbH
Carl-Legien-Str. 30
63073 Offenbach/Main, Germany
Email: stefan.menzel@honda-ri.de

***Abstract*—The performance of design optimizations which target the improvement of certain physical aspects of real world objects like e.g. in the automotive or aeronautical domain depends on the efficient interplay of optimization algorithm, evaluation method and shape representation. For the development of complex aerodynamic components, evolutionary algorithms as global stochastic optimization algorithms have been successfully coupled to shape morphing methods. Instead of a direct representation of the shapes' boundary, shape morphing methods like free-form deformation (FFD) apply scalable changes to a baseline prototype using a moderate number of parameters mapped to control point movements. The initial spatial arrangement of the control points influences strongly the design flexibility and the optimization performance in combination with the normal distributed mutation operator in evolutionary optimization algorithms. In the present paper, a method is proposed to support the generation process of initial FFD control volumes which is usually carried out manually in practice. The method is based on the concept of evolvability which is considered as the property of initial control volumes to generate favorable design variations within a moderate number of iterations while avoiding unfeasible mutations. We introduce mathematically translational design variability, mutational design variability and the central robust control volume as key features to compute an evolvable distribution of control points. In target shape matching experiments using an evolutionary strategy, the performance for different configurations of evolvability-tuned initial control volumes is shown empirically.**

Keywords-evolvability, robustness, free-form deformation, control volume, evolutionary design optimization

I. INTRODUCTION

Evolutionary design optimization is successfully applied to improve physical aspects of real world objects, like car, wing and airfoil shapes in an optimization process driven by population based evolutionary search algorithms [1], [2], [3], [4]. Due to the availability of computing resources, stochastic optimization methods like evolutionary algorithms become more and more popular over deterministic approaches like gradient based methods, since they can handle noisy search landscapes and overcome local optima. Evolutionary algorithms mimic the concepts of biological evolution and can be applied to fine tune existing shapes, as well as to discover unexpected solutions out of the scope of human experience. Besides the principles of selective breeding, recombination and random mutations, other biological principles are investigated in evolutionary computing as well [5].

Robustness and evolvability are identified to be key features for the success of evolution [6], [7]. Robustness is favored by evolution and is an important property of biological systems, since it quantifies the ability of living systems to maintain performance in the face of perturbations and uncertainty [8], [9]. In contrast, evolvability addresses the ability to produce ample genetic variation and evolutionary innovations in highly dynamic environments [7]. The relationship between robustness and evolvability explains how evolution can evolve millions of viable diverse species and how evolution can transfer perturbing external influences and random mutations into beneficial improvements and novel functions [10].

In [11], the concept of evolvability is introduced into the setup process of an evolutionary design optimization which utilizes shape morphing methods as representation. Combining shape morphing like free-form deformation (FFD) as prominent representative with an evolutionary algorithm allows the efficient optimization of complex components of real-world objects [1]. FFD provides a fair trade-off between parameter number and shape flexibility and unfolds its full strength in design optimizations using Computational Fluid Dynamics (CFD) or Finite Element Analysis (FEA) methods due to the capability to deform geometry and numerical grid simultaneously.

Analogously to [11], in the present paper we also consider evolvability in the sense of the capacity of a system to being able to produce favorable phenotypic variations of a design within a moderate number of generations while avoiding non-feasible mutations. We provide an extended approach for FFD control volumes consisting of an arbitrary number of control points by introducing key features as translational design variability, mutational design variability and the central robust control volume mathematically. While translational design variability is a spline inherent characteristic, mutational design variability is closely linked to evolutionary algorithms. The central robust control volume finally configures control points in a way that unfeasible mutations are avoided. Combining these three features returns control volumes which are tuned to evolvability following the above given definition [12].

The paper is organized as follows. In section II, FFD as state-of-the-art shape morphing algorithm is introduced in the area of design optimization. Section III reviews the idea of evolvable initial FFD control volumes which is utilized in section IV to derive translational design variability, mutational design variability and the central robust control volume mathematically for an arbitrary number of control points. Section V presents empirical results of evolutionary target matching optimizations using evolvable FFD control volumes followed by concluding remarks in section VI.

II. Free-Form Deformation in Design Optimization

In almost any context of optimization the problem representation has a major influence on the convergence of the optimization algorithm and the resulting solution of the optimization process. In the context of design optimization considered, the shape representation determines the manifold of shape modifications and the dimensionality of the search space.

Thus, the choice and setup of the shape representation for a given use case are an important task with strong influence on the overall success of the optimization process. In the present evolutionary design optimization setup, FFD [13], [14] is used as shape morphing method to represent the geometry. In contrast to a direct representation of the shapes' surface like B-spline surfaces, boundary and constructive solid geometry representations, FFD is used to parameterize a portion of world space and in turn an existing baseline prototype located therein. Hence, FFD can be applied to indirectly represent complex shapes with holes or sharp edges. Especially in design optimization scenarios, at which the performance evaluation of the shape relies on features extracted from CFD or FEA simulations, FFD unfolds its power by parameterizing the numerical grid along with the object. This reduces the computational effort for evaluating the performance index of proposed shapes, as the numerical grid is kept omitting expensive mesh generation algorithms. The main idea behind FFD is illustrated in Fig. 1.

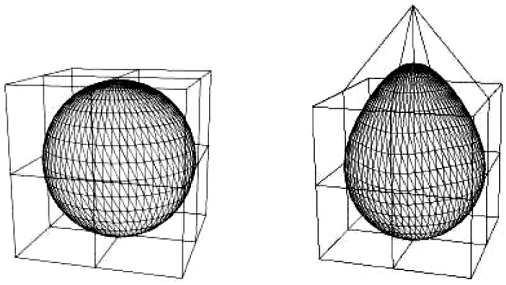

Figure 1. Free-form deformation. Left: Initial geometry and control volume. Right: Deformed geometry and control volume, taken from [15].

FFD is a powerful sculpturing tool for deforming solid geometric models in a free-form manner and has been successfully applied to various optimization scenarios [1], [15]. In the present case, FFD relies on B-splines [16] used to parameterize the world space. From design optimization point of view, FFD corresponds to imposing a parametric B-spline patch onto a portion of world space and linking distortions in the spline patch to object vertices and is formulated as a mapping, from undeformed world space, through the spline parameter space, to deformed world space. The mapping from undeformed world space to spline parameter space is called embedding or freezing. The control polygon, used to configure the spline patch at embedding, is called initial control volume and the mapping from spline parameter space back to world space is called deforming. Deformations are modeled by modifying a subset of the control points inside the initial control volume, which then is called deformed control volume.

In general, the number of control points moved to obtain the deformed control volume determines the dimensionality of the search space and the manifold of possible shape manipulations. By using a subset of the control points as optimization parameters, FFD is coupled to an optimization scenario.

For examinations in this report, a simplified case of FFD in one dimensional world space is considered. Control volumes P consist of n+1 = 5 ordered control points (p_0, p_1, p_2, p_3, p_4) on the real line. A control volume P, the clamped equidistant knot vector U = (0, 0, 0, 0, 0.5, 1, 1, 1, 1) and the spline degree p = 3 are needed to define the B-spline patch following [16] by

$$F_p(u \in [0,1]) = \sum_{i=0}^{n} N_i(u) \cdot p_i \tag{1}$$

used for embedding and deforming, where the B-spline basis functions $N_i(u) := N_{i,3}$ (i = 0,…, n) are recursively defined by

$$N_{i,p} = \frac{u - u_i}{u_{i+p} - u_i} N_{i,p-1} + \frac{u_{i+p+1} - u}{u_{i+p+1} - u_{i+1}} N_{i+1,p-1} \tag{2}$$

$$N_{i,0} = \begin{cases} 1 & , \text{if } u \in [u_i, u_{i+1}] \\ 0 & , \text{otherwise} \end{cases} \tag{3}$$

Embedding and deforming using the above FFD setup is explained at one example in the following. A simplified shape is composed of two object points $q_1 = 0.375$ and $q_2 = 0.625$ on the real line. The initial control volume is given by P = (0, 0.25, 0.5, 0.75, 1). To embed both object points into spline parameter space, the inverse function $u = F^{-1}(q)$ has to be computed for q_1 and q_2. This yields the spline parameters $u_1 \approx 0.333$ and $u_2 \approx 0.667$, which are used in the deformation step. The embedding is illustrated in Fig. 2.

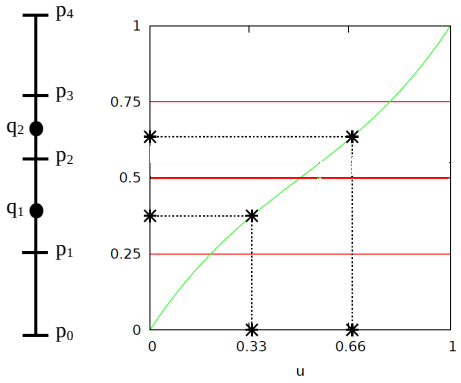

Figure 2. Free-form deformation. Initial geometry and control volume.

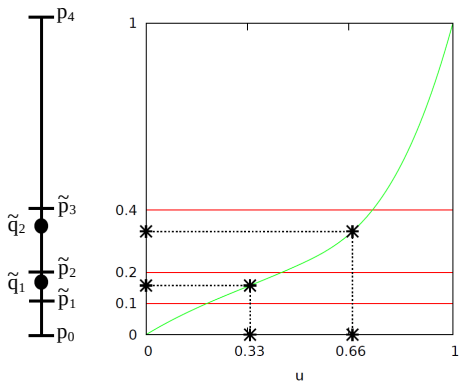

Figure 3. Free-form deformation. Deformed geometry and control volume.

Deformed object points are obtained by computing $\tilde{q} = F_{\tilde{P}}(u)$ for u_1 and u_2 using for example the deformed control volume $\tilde{P} = (0, 0.1, 0.2, 0.4, 1)$, which is obtained by moving interior control points of the initial control volume according

$$\tilde{P} = P + \Delta P \tag{4}$$

$$= (p_0, p_1 + \Delta p_1, p_2 + \Delta p_2, p_3 + \Delta p_3, p_4) \tag{5}$$

$$= (p_0, \tilde{p}_1, \tilde{p}_2, \tilde{p}_3, p_4) \tag{6}$$

The deformed shape represented by the two object points $\tilde{q}_1 \approx 0.15$ and $\tilde{q}_2 \approx 0.33$ is illustrated in Fig. 3. Based on this simplified setup of FFD, evolvable control volumes are explained in the next section.

III. Evolvable Initial FFD Control Volumes

Robustness and evolvability are considered as important properties of biological and technical systems, which preserve the function of the system under and the adaptation of the system to perturbing influences and changing environmental conditions. In contrast, from a mutational point of view to evolution evolvability of biological and computational systems can be seen as the ability of random variants to sometimes produce improvement. This ability critically depends on the way how genetic variation is mapped onto the phenotypic variation, the so-called genotype-phenotype mapping, and is known as the representation problem [5]. In [7] the genotype-phenotype mapping is used to identify robustness and evolvability of genotypes and phenotypes of ribonucleic acid sequences and structures in a quantitative manner and it is shown that robustness can support evolvability.

In [11] the transfer of the concepts of evolvability to the FFD representation in evolutionary design optimization is proposed. Evolvability is considered in the sense of the capacity of a system to produce favorable phenotypic variations of a design within a moderate number of generations while avoiding non-feasible mutations which is also our reference in the present paper. The proposed method allows the computation of evolvable initial FFD control volumes by implementing the distinction between genotypes and phenotypes in a many-to-one genotype-phenotype-mapping since it has been shown for biological systems that a representation which generates highly robust structures promotes evolvability [7].

An initial control volume P which has been computed based on the proposed method is used for embedding the shape in spline parameter space in an optimal way related to a given use case of design optimization. To study the effects of evolvable FFD control volumes a simplified geometry and FFD setup has been chosen in [11]. Instead of considering a whole shape, only one point of interest $q \in (p_0, p_3)$ within a one-dimension FFD control volume comprising 4 control points (p_0, p_1, p_2, p_3) has been selected. The point of interest is chosen by an expert and marks an important region on the shape. The point of interest is considered to be related to the present use case and hence to the underlying optimization problem. Given an initial control volume P, q receives its associated spline parameter $u = F_P^{-1}(q)$.

Benchmark evolutionary optimization runs have been carried out in [11] underlining that evolvable control volumes in average converge faster and reach a better final fitness value. The results are derived from moving q to a randomly chosen target point t, whereat the control points $\tilde{p}_1$ and $\tilde{p}_2$ are used as optimization parameters in $| F_{\tilde{P}}(u) - t | \rightarrow \min_{\tilde{P}}$ keeping p_0 and p_3 constant. Keeping p_0 and p_3 constant enables a seamless merge between deformed and undeformed regions in world space, since $F_P(0) = p_0$ and $F_P(1) = p_3$ which is additionally strengthened by the C0 and C1 continuity of the B-spline functions. Given an initial control volume P and the point of interest q, evolvability E raises from structural robustness S and design variability V and is defined by $E = S \cdot V$ to allow basic empirical studies, although it is a multi-objective problem. This quality measure E is presented for initial control volumes in one dimensional design optimization on the real line. It can be used for the automated setup of evolvable initial control volumes for design optimization. Alongside the biological standpoint, the proposal of evolvable initial control volumes is introduced which allows the generalization to the construction of three dimensional initial control volumes.

Design variability V is obtained by moving control points p_1 and p_2 to the maximum left and right extents, which defines the extents of world space reachable by the point of interest q. This can be modeled by two deformed control volumes given by $\tilde{P}_1 = (0, 0, 0, 1)$ and $\tilde{P}_2 = (0, 1, 1, 1)$. Design variability then is given by

$$V = \frac{F_{\tilde{P}_2}(u) - F_{\tilde{P}_1}(u)}{p_3 - p_0}. \tag{7}$$

Structural robustness S is obtained by counting distinct deformed control volumes $\tilde{P}$, which yield only small changes to the point of interest ($|F_{\tilde{P}}(u) - q| \leq \varepsilon$). Structural robustness is given by

$$S = \frac{1}{|X|} \cdot \sum_{\tilde{P} \in X} \begin{cases} 1 & , \text{if } |F_{\tilde{P}}(u) - q| \leq \varepsilon \\ 0 & , \text{otherwise} \end{cases} \tag{8}$$

where X is a discrete set of deformed control volumes, for example a full sampling of $p_0 \le \tilde{p}_1 \le \tilde{p}_2 \le p_3$ with a small step size. A similar approach to variability and robustness involving discrete Boolean mappings is proposed in [17].

In the following the concept of evolvable initial control volumes developed in [11] is viewed from a geometrical perspective. This allows the examination of the performance of (1+1) evolutionary strategies [18] according the definition of evolvability given above. Furthermore, a way to select initial control volumes avoiding unfeasible mutations is presented.

IV. Evolvable Control Volumes for Arbitrary Numbers of Control Points

In section III we reviewed the concept of evolvable initial FFD control volumes which has been introduced in [11] where it has been shown that these control volumes in average provide a better final fitness value and converge faster. In this section we will explain this mathematically by embedding it in the context of evolutionary optimization.

From a practical point of view, an application of FFD in design optimization scenarios requires physically plausible deformations of the shape, especially when a numerical grid and the shape are deformed together. In [19] this is identified as the self-intersection problem and is reduced to the injectivity of the underlying B-spline patch. To guarantee plausible deformations, the set of deformed control volumes $\Pi(P)$ build on top of the initial control volume P is considered to produce valid deformations in this sense. Given an initial control volume $P = (p_0, p_1, p_2, p_3, p_4)$ with 5 ordered control points $p_0 < p_1 < p_2 < p_3 < p_4$ on the real line exemplary shown in Fig. 2, where the first and the last control point are kept fix, the set of valid deformed control volumes is then defined as

$$\Pi(P) = \{(p_0, \tilde{p}_1, \tilde{p}_2, \tilde{p}_3, p_4) : p_0 \le \tilde{p}_1 \le \tilde{p}_2 \le \tilde{p}_3 \le p_4\}. \quad (9)$$

Since B-spline curves, used in the present FFD setup, are located in the convex hull of four following control points [16], control volumes with ordered control points provide injective mappings $F_P(u)$. Additionally, allowing control points $\tilde{p}_1$, $\tilde{p}_2$ and $\tilde{p}_3$ to be equal at deforming enables regions of world space to be reduced to one single point. Control points p_0 and p_4 stay fixed.

In the following, two concepts called translational design variability V_T and mutational design variability V_M are introduced. The definitions of V_T and V_M are inspired by the first part of the evolvability definition given above for initial control volumes in the sense of the capacity of a system to produce favorable phenotypic variations of a design within a moderate number of generations. This involves the control of the performance of a (1+1) evolutionary strategy (ES), used as benchmark system in the present paper. It is shown that mutational design variability V_M is related to structural robustness S introduced in [11] and significantly reduces the computational effort to determine evolvable initial control volumes. To tackle the avoidance of non-feasible mutations, afterwards the concept of the central robust control volume $\hat{P}$ is introduced.

A. Translational Design Variability

Translational design variability V_T is related to the set of points in world space, reachable by the point of interest and is related to design variability V defined in [11]. V_T corresponds to the sum of B-spline basis functions of control points p_1, p_2 and p_3 used as optimization parameters. Simplifying (7) yields

$$V_T = N_1(u) + N_2(u) + N_3(u). \quad (10)$$

Moving control points $\tilde{p}_1$, $\tilde{p}_2$ and $\tilde{p}_3$ to its maximum extents, bounded by p_0 and p_4 also moves the point of interest q embedded at u to its maximum extents. V_T can be imagined like a scaling between control point displacement and the resulting displacement induced to the point of interest q. The higher the value of V_T the more points are reachable by the point of interest. The value of V_T indicates also the sensitivity of the spline to the point of interest. Fig. 4 top shows a plot of V_T depending on the spline parameter q received at embedding.

B. Mutational Design Variability

Mutational design variability V_M is related to the performance of the (1+1)–ES according the definition of evolvability in the sense of the capacity of a system to produce favorable phenotypic variations of a design within a moderate number of generations as given above. Favorable phenotypic variation is considered to converge towards near target points or to reach the vicinity of far target points. Mutational design variability V_M scales the variance of random mutations of control points Δp_i obtaining the variance of the random displacement Δq of the point of interest. Under the assumption of identically independent normal distributed mutations of control points $\Delta p_i \sim N(0, \sigma^2)$, the distribution of $\Delta q = \sum_{i=1}^{n} N_i(u) \cdot \Delta p_i$ is given by $\Delta q \sim N(0, V_M^2 \cdot \sigma^2)$ and

$$V_M^2 = \sum_{i=0}^{n} N_i(u)^2. \quad (11)$$

Thus, mutational design variability V_M can be seen as the scaling of the variance of the mutation step size σ in the normal distributed mutation operator in (1+1)–ES. V_M is related to structural robustness S introduced in [11]. Equivalent to counting the number of control volumes from a discrete set X following (8), S can be measured as a volume. Considering q being embedded at u, two planes which describe the positions of control points $\tilde{p}_1$, $\tilde{p}_2$ and $\tilde{p}_3$ for the deformed point of interest to be at $\tilde{q}_1 = q \pm \varepsilon$ can be derived from (1) according

$$N_1\tilde{p}_1 + N_2\tilde{p}_2 + N_3\tilde{p}_3 = q - N_0p_0 + N_4p_4 \pm \varepsilon = \bar{q} \pm \varepsilon \quad (12)$$

Structural robustness S then is given as the volume of deformed control volumes $(p_0, \tilde{p}_1, \tilde{p}_2, \tilde{p}_3, p_4) \in \Pi(P)$ lying between the planes defined in (12), whereat $\bar{q} \pm \varepsilon$ are constants. It can be derived that mutational design variability V_M is indirectly proportional to the distance d of the two planes [12]

$$d = \frac{2 \cdot \varepsilon}{\sqrt{N_1^2 + N_2^2 + N_3^2}} = \frac{2 \cdot \varepsilon}{V_M}. \quad (13)$$

This means, one dimension of the volume of structural robustness S is related to mutational design variability, which in turn is related to the performance of the normal distributed mutation operator of the (1+1)–ES.

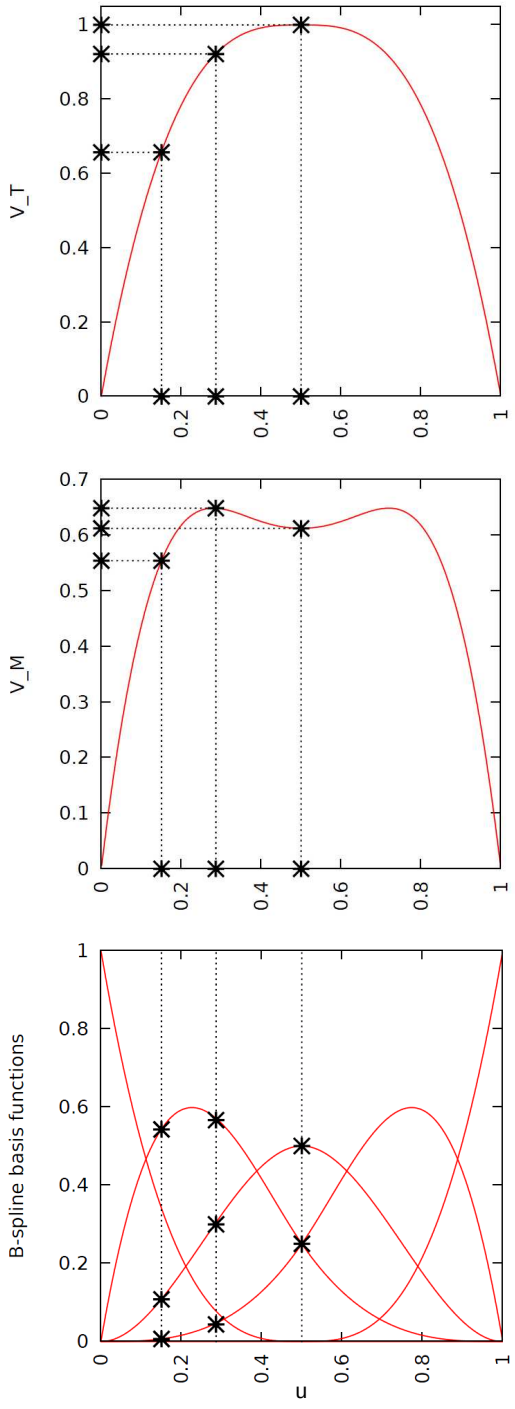

Figure 4. Top: Translational design variability V_T. Center: Mutational design variability V_M. Bottom: B-spline basis functions according FFD set-up described in section 2. Dotted lines show the configurations of P_1, P_2 and P_3.

Embedding the point of interest with low mutational design variability V_M increases the probability to make small steps Δq in world space. This yields a better performance to converge towards a target point t being in the vicinity of q. Embedding with high mutational design variability V_M increases the probability to make large steps Δq in world space. This yields a better performance to reach the vicinity of a target point t far away from q.

The performance of the random normal distributed mutation operator in (1+1)–ES with mutation step size σ is measured as the number of iterations needed to match a target point t in the optimization problem $| F_{\tilde{P}}(u) - t | \rightarrow \min_{\tilde{P} \in \Pi(P)}$, where $p_0 = 0$ and $p_4 = 1$ are kept fix. Experiments and results are presented in section 5.

C. *Central Robust Control Volume*

Translational design variability V_T and mutational design variability V_M capture aspects of evolvability due to enabling favorable phenotypic variation in the modifications of the point of interest q. However, the definition of evolvability of initial control volumes considered in the present paper also includes the avoidance of unfeasible mutations as a requirement. To regard the avoidance of non-feasible mutations, the concept of the central robust control volume $\hat{P}$ is introduced. The idea is to determine $\hat{P}$ to have a large distance to the boundary of the set of valid deformed control volumes $\Pi(P)$ to allow a maximum of possible feasible mutations during the evolutionary optimization.

To prepare the calculation, an initial control volume P has to be supplied. P which has to be a valid control volume with respect to injectivity serves as the basis for the definition of $\Pi(P)$ and has the desired properties V_T and V_M which are adjusted to the present use case, e.g. by selecting u for one point of interest q. P is updated iteratively to obtain $\hat{P}$ preserving u, V_T and V_M with respect to a given point of interest q. By $\hat{P}$ having a large distance to the boundary of $\Pi(P)$, the (1+1)–ES can walk a far distance on the fitness landscape without encountering unfeasible mutations. Since the optimal walking direction in general is not known, it is attempted to center $\hat{P}$ in $\Pi(P)$. To do so a way has to be found, which moves P in $\Pi(P)$ preserving the spline parameter u, at which q is embedded. This is accomplished by using linear algebra. Therefore, (1) is transformed to matrix notation given by

$$N_1 p_1 + N_2 p_2 + N_3 p_3 = q - N_0 p_0 + N_4 p_4 \quad (14)$$

$$\Rightarrow \begin{pmatrix} N_1 & N_2 & N_3 \end{pmatrix} \cdot \begin{pmatrix} p_1 \\ p_2 \\ p_3 \end{pmatrix} = \bar{q} \quad (15)$$

$$\Rightarrow \bar{N} \cdot \bar{P} = \bar{q} \quad (16)$$

Considering $\bar{N}$ to be a matrix, the deformed control volume $\tilde{P} = P + \Delta P$ preserves q if and only if $\bar{N} \cdot \Delta P = 0$. Mathematically, this defines the null space [20], [21] of $\bar{N}$. The null space is given by the kernel $\mathrm{Ker}(\bar{N})$. The column vectors of

$\mathrm{Ker}(\bar{N})$ have to be an orthonormal basis of the null space and can be obtained using singular value decomposition. Finally, $\tilde{P}$ is given by

$$\tilde{P} = P + \Delta P = P + \mathrm{Ker}(\bar{N}) \cdot \begin{pmatrix} \omega_1 \\ \omega_2 \end{pmatrix} \tag{17}$$

where ω_1 and ω_2 are parameters of the solution to the underdetermined linear system given in (16). Any choice of $(\omega_1, \omega_2)^T$ determines a control volume, which preserves the desired properties. The only thing which has to be taken care of, is that the resulting control volume $\tilde{P}$ lies inside $\Pi(P)$ for it to satisfy the validity constraint, i.e. injectivity, as explained above.

To obtain $\hat{P}$ iteratively, $\hat{P}$ is initialized to P at the beginning and a set of control volumes Y containing s_1 pairs of opposite points $\tilde{P}_1, \tilde{P}_2 \in Y$ on the boundary of $\Pi(P)$ is determined. To determine the opposite control volumes on the boundary, for each pair a uniform distributed point on the unit circle $(\omega_1, \omega_2)^T$ is drawn, which is used to define a line in the null space of $\bar{N}$ given by

$$\tilde{P} = \hat{P} + b \cdot \mathrm{Ker}(\bar{N}) \cdot \begin{pmatrix} \omega_1 \\ \omega_2 \end{pmatrix} \tag{18}$$

$\tilde{P}_1, \tilde{P}_2 \in Y$ are obtained by doing a binary search on b in both directions of the line. Given Y containing k control volumes $\tilde{P}$, $\hat{P}$ is updated by the sum of the points in Y weighted by the distance to all other points in Y according

$$\hat{P} := \frac{1}{D} \cdot \sum_{i=1}^{k} \left[d(\tilde{P}_i, Y) \cdot \tilde{P}_i \right] \tag{19}$$

$$D = \sum_{i=1}^{k} d(\tilde{P}_i, Y) \;,\; d(x, Y) = \sum_{i=1}^{k} \left\| \tilde{P}_i - x \right\| \tag{20}$$

This procedure is repeated for s_2 times until convergence. Since $\Pi(P)$ is convex, $\hat{P}$ is always a valid control volume. The idea is that points being far away from other boundary points in Y receive a large weight moving $\hat{P}$ away from the boundary. By the distances between the points being similar, $\hat{P}$ will not change much anymore. For future work, a proper definition of a centroid of a set may be applied. For this, the boundary of $\Pi(P)$ intersected with the null space has to be determined explicitly. This is a hard geometrical task, especially in the three dimensional case of FFD.

D. Generalized Algorithm for 3D Arbitrary Control Volumes

The matrix notation introduced along with the calculation of the central robust control volume can directly be generalized to the three dimensional case and for arbitrary numbers of control points. Many points of interest can be introduced by adding equations to the $\bar{N}$ matrix, but the linear system has to stay underdetermined for $\mathrm{Ker}(\bar{N})$ to exist. The set of valid deformed control volumes is defined as the set of lattices, which have convex cells composed of eight control points.

The algorithm for calculating evolvability-tuned initial FFD control volumes is as follows.

Algorithm 1. Evolvable initial FFD control volumes

(a) Select points of interest q on shape
(b) Select for each point of interest a spline parameter u according to V_T and V_M using (10) and (11).
(c) Find an arbitrary valid initial control volume P.
(d) Calculate central robust control volume:
  (d1) Calculate $\mathrm{Ker}(\bar{N})$.
  (d2) $\hat{P} \leftarrow P$
  (d3) for $i = 0 \rightarrow s_1$ do
    for $j = 0 \rightarrow s_2$ do
      $\omega \leftarrow \mathrm{RandomUniformSphere}(\bar{n})$,
        $\bar{n}$ specifies the colomn rank of $\mathrm{Ker}(\bar{N})$
      $\tilde{P}_- \leftarrow \hat{P} - b_- \cdot \mathrm{Ker}(\bar{N}) \cdot \omega^T$
      $\tilde{P}_+ \leftarrow \hat{P} + b_+ \cdot \mathrm{Ker}(\bar{N}) \cdot \omega^T$
        (b_- and b_+ are subject to binary search)
    end for
    Update $\hat{P}$ using (19) and (20)
  end for
  return $\hat{P}$

To illustrate preliminary results two three dimensional initial control volumes with 5x5x5 control points have been calculated and the resulting initial control volumes as well as the setup is summarized in Fig. 5.

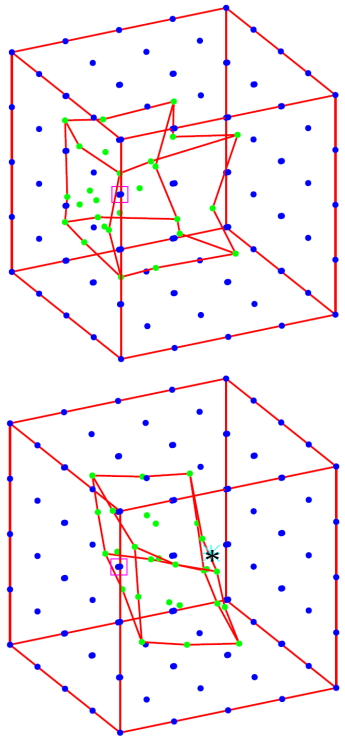

Figure 5. Three dimensional evolvable initial control volumes composed of 5x5x5 control points. Top: One point of interest q = (0.3, 0.45, 0.4) (□). Inner control points were moved so that $F_P(0.5, 0.5, 0.5) = q$. Then the central robust control volume $\hat{P}$ was computed. Bottom: Two points of interest at $q_1 = (0.3, 0.35, 0.4)$ (□) and $q_2 = (0.65, 0.6, 0.55)$ (*). Control points were moved so that $F_P(0.28, 0.28, 0.28) = q_1$ and $F_P(0.72, 0.72, 0.72) = q_2$. Afterwards the central robust control volume $\hat{P}$ was computed.

V. EXPERIMENTS

We conducted experiments for FFD control volumes which follow the layout described in section 2 to perform statistical analysis. Three different initial control volumes P1, P2 and P3, which result in different spline parameters u concerning one point of interest q, are selected. The point of interest is chosen as $q = 0.25$. P1 = (0, 0.325, 0.625, 0.800, 1), P2 = (0, 0.175, 0.400, 0.600, 1) and P3 = (0, 0.100, 0.200, 0.500, 1) are chosen by probing to obtain three different values for V_T and V_M.

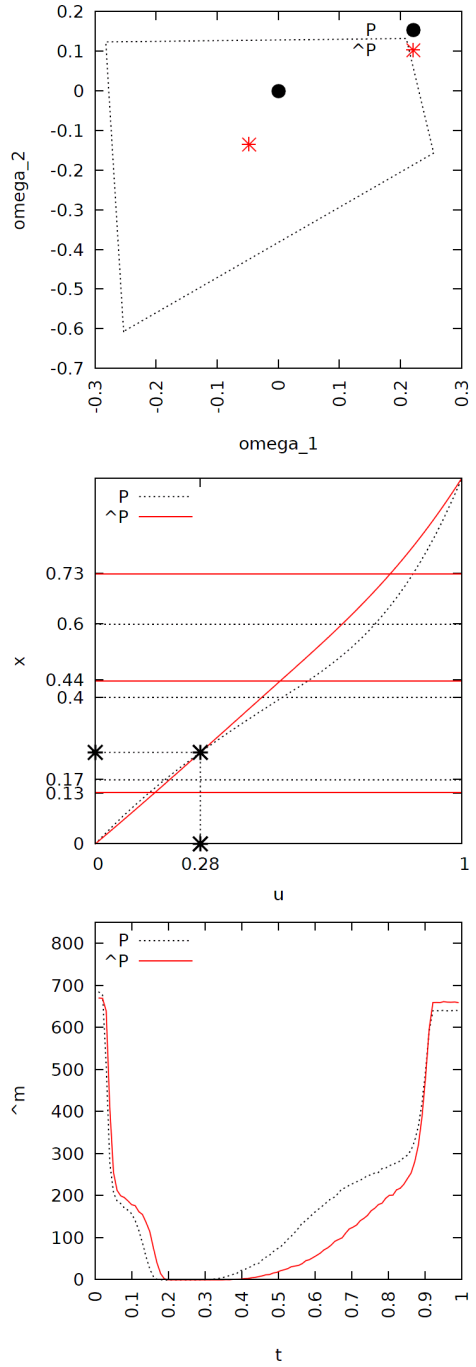

Figure 6. Top: Null space of $\bar{N}$ intersected with $\Pi(P)$. Points show difference between P_2 and $\hat{P}_2$. Middle: Embedding mappings $F_{P/\hat{P}}$ (u) resulting from P_2 and $\hat{P}_2$. Bottom: Mean unfeasible mutations $\hat{m}$.

Embedding q into the initial control volume yields $u_1 \approx 0.15$, $u_2 \approx 0.29$ and $u_3 \approx 0.5$. Translational design variability is calculated according (10) to $V_T(u_1) \approx 0.66$, $V_T(u_2) \approx 0.92$, $V_T(u_3) = 1$, and mutational design variability according (11) to $V_M(u_1) \approx 0.55$, $V_M(u_2) \approx 0.65$, $V_M(u_3) \approx 0.61$. The configuration of B-spline basis functions $N_{0\ldots4}(u)$, V_T and V_M is shown in Fig. 4.

For each of the initial control volumes P_1, P_2 and P_3 with the desired properties the optimal starting solution $\hat{P}_1$, $\hat{P}_2$ and $\hat{P}_3$ is calculated according section 4. $\hat{P}_1$ and $\hat{P}_3$ do not differ from P_1 and P_3 much, but P_2 changes to $\hat{P}_2 \approx (0, 0.138, 0.446, 0.738, 1)$. The difference between P_2 and $\hat{P}_2$ in the null space of $\bar{N}$ is shown in Fig. 6 top. The corresponding embedding mappings are shown in Fig. 6 middle. Computing $\hat{P}_2$ from P_2 centers the initial control volume in the null space of $\bar{N}$ intersected with $\Pi(P)$. This moves control points, to have a large distance to each other and decreases the probability for unfeasible mutations.

To measure the performance of the (1+1)–ES for the three different initial control volumes $P_{1/2/3}$ in the optimization problem $|F_{\tilde{P}}(u) - t| \rightarrow \min_{\tilde{P} \in \Pi(P)}$, a full sampling of target points $t = 0.01, 0.02, \ldots 0.99$ is made. For each target point t, a (1+1)–ES with mutation step size $\sigma = 0.01$ is run for 1000 iterations. For statistical observations, each optimization run is repeated for 5000 times.

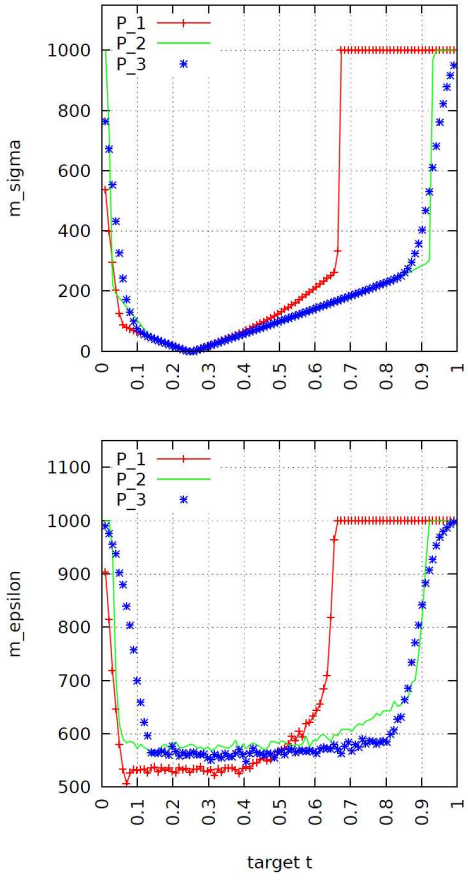

Figure 7. Top: Mean iterations needed to reach fitness value in $[0, \sigma)$ matching t with q. Bottom: Mean iterations needed to reach fitness value in $[0, \varepsilon)$ matching t with q.

To show the decrease of unfeasible mutations when starting optimization from the central robust control volume $\hat{P}_2$ the mean number of unfeasible mutations $\hat{m}$ is obtained for each target t and shown in Fig. 6 bottom. Starting from $\hat{P}$ results in less unfeasible mutations compared to starting from P. The performance of reaching the vicinity of a target t is measured as the mean number of iterations needed to get a fitness value $f < \sigma$ and shown in Fig. 7 top. According to the higher V_T, P_2 and P_3 outperform P_1 in reaching the vicinity of far targets. The difference between P_2 and P_3 is only minor. P_2 has a better performance for targets near p_0 and p_4, however P_3 can reach all targets. The performance of converging towards a target t is measured as the mean number of iterations needed to get a fitness $f < \varepsilon = 10^{-5}$ starting from a random fitness value $f < \sigma$. P_1 outperforms P_2 and P_3 in converging towards reachable targets $t \leq 0.5$. For targets $t > 0.5$ the performance of P_1 decreases, since control points are near each other yielding many unfeasible mutations. P_3 is slightly faster than P_2, since mutational design variability V_M is lower. Invalid mutations, which yield $\tilde{P} \notin \Pi(P)$, are also counted within m_σ and m_ε.

VI. CONCLUSION

In the present paper we extended the idea of designing initial control volumes for FFD-based evolutionary optimizations utilizing the concept of evolvability as proposed in [11]. Deeper mathematical insights are given which are used to derive the applicability for arbitrary numbers of control points. We rely on evolvability as the property of initial control volumes to generate favorable design variations within a moderate number of iterations avoiding unfeasible mutations. A (1+1)–ES with static step size has been picked as benchmark system, since it reflects the behavior of the normal distributed mutation operator best.

Alongside the biological standpoint from which the theory of evolvability arises, a mathematical view implies the distinction of design variability in translational and mutational traits. Translational design variability V_T is a spline inherent characteristic. Since structural robustness S as introduced in [11] has been shown to be associated to mutational design variability V_M, the calculations involved in generating evolvable initial control volumes are simplified omitting the expensive sampling of initial control volumes. The avoidance of unfeasible mutations is accomplished by centering the starting volume in the set of valid control volumes, introducing the concept of the central robust control volume $\hat{P}$. The calculations involved in generating evolvable initial control volumes have been transferred to the 3D case of FFD. The computational effort to obtain translational and mutational design variability scales well, since only B-spline basis functions have to be evaluated. However, the problem lies in finding an initial control volume P, which has the desired properties V_T and V_M. This is so far accomplished by an optimization of control points moving the point of interest to the desired spline coordinate u. After a valid control volume $P \in \Pi(P)$ is found, the central robust control volume $\hat{P}$ can be computed as described in section 4.

The impact of V_M on the performance of moving the point of interest to desired target points has been shown. However, the value of V_M for large control volumes oscillates around a constant, which does not supply a great scope to tuning. By using arbitrary knot vectors for configuring B-spline basis functions, this scope can be extended. This has impact on the morphing of the surrounding world space and thus on the movement of the remaining object points not in the regions marked by the point of interest. The impact of arbitrary knot vectors on the whole design optimization process has to be carried out separately and may be addressed in future work.

REFERENCES

[1] S. Menzel, and B. Sendhoff, "Representing the change – Free form deformation for evolutionary design optimization," in Evolutionary Computation in Practice, Springer, Berlin, pp. 63-86, 2008.

[2] J. A. Samareh, "Aerodynamic shape optimization based on free-form deformation," in 10th AIAA/ISSMO Multidisciplinary Analysis and Optimization Conference, 2004.

[3] M. Nashvili, M. Olhofer, and B. Sendhoff, "Morphing methods in evolutionary design optimization," in H.-G. Beyer, editor, Proceedings of the Genetic and Evolutionary Computation Conference - GECCO, ACM Press, pp. 897–904, 2005.

[4] S. Menzel, M. Olhofer, and B. Sendhoff, "Evolutionary design optimization of complex systems integrating Fluent for parallel flow evaluation," in Proceedings of EACC, pp. 279-289, Frankfurt, 2005.

[5] G. P. Wagner, and L. Altenberg, "Complex adaptations and the evolution of evolvability," Evolution, Vol. 50, No. 3., 1996.

[6] H. Kitano, "Biological robustness," Nature Review Genetics, vol. 5, pp. 826-837, 2004.

[7] A. Wagner, "Robustness and evolvability: a paradox resolved," in Proc. R. Soc. B, vol. 275, pp. 91-100, 2008.

[8] J. A. de Visser et al., "Perspective: Evolution and detection of genetic robustness," Evolution, Vol. 57, No. 9, pp. 1959–1972, 2003.

[9] J. Stelling, U. Sauer, Z. Szallasi, F. J. Doyle, and J. Doyle, "Robustness of cellular functions," Cell, Vol. 118, No. 6, pp. 675-685, 2004.

[10] A. Wagner, "Robustness, evolvability, and neutrality," FEBS Letters, Vol. 579, No. 8, pp. 1772-1778, 2005.

[11] S. Menzel, "Evolvable free-form deformation control volumes for evolutionary design optimization," in IEEE Congress on Evolutionary Computation, IEEE, New Orleans, pp. 1388-1395, 2011.

[12] H. Lehmann, "Evolvability as concept for the optimal design of free-form deformation control volumes," Master Thesis, TU Bergakademie Freiberg, 2011.

[13] T. W. Sederberg, and S. R. Parry, "Free-form deformation of solid geometric models," Computer Graphics, 20(4), pp. 151-160, 1986.

[14] S. Coquillart, "Extended free-form deformation: a sculpturing tool for 3D modelling," Computer Graphics, 24(4), pp. 187-196, 1990.

[15] E. C. Perry, S. E. Benzley, M. Landon, and R. Johnson, "Shape optimization of fluid flow systems," in Proceedings of ASME FEDSM'00, Boston, 2000.

[16] L. Piegl, and W. Tiller, "The NURBS book," 2nd edition, Springer, Berlin, 1997.

[17] Y. Jin, R. Gruna, I. Paenke, and B. Sendhoff, "Evolutionary multi-objective optimization of robustness and innovation in redundant genetic representations," in 2009 IEEE Symposium on Computational Intelligence in Multi-Criteria Decision-Making (IEEE MCDM 2009), IEEE Press, pp. 38-45, 2009.

[18] I. Rechenberg, "Evolutionsstrategie – Optimierung technischer Systeme nach Prinzipien der biologischen Evolution," Fommann-Holzboog, 1973.

[19] J. E. Gain, and N. A. Dodgson, "Preventing self-intersection under free-form deformation," IEEE Transactions on Visualization and Conputer Graphics, Vol. 7, No. 4, pp. 289-298, 2001.

[20] C. Meyer, "Matrix analysis and applied linear algebra," SIAM: Society for Industrial and Applied Mathematics, 2001.

[21] S. Axler, "Linear algebra done right," Undergraduate Texts in Mathematics, Springer-Verlag, 2nd edition, New York, 1997.